PHYSICAL REVIEW B VOLUME 56, NUMBER 17 1 NOVEMBER 1997-I

ARTICLES

Stacking faults in magnesium

N. Chetty
Department of Physics, Brookhaven National Laboratory, Upton, New York 11973-5000
*and Department of Physics, University of Natal, Private Bag X01, Scottsville 3209, South Africa**

M. Weinert
Department of Physics, Brookhaven National Laboratory, Upton, New York 11973-5000

(Received 30 May 1997)

The energetics of various low-energy intrinsic, extrinsic, and twinlike stacking fault configurations in hexagonal-close-packed magnesium are determined from first-principles calculations. To zeroth-order, the ordering of the energies can be understood in terms of the number of fcc-like planes in the sequence of close-packed planes. However, such a simple model fails to quantitatively reproduce the calculated energies of the faults. We propose a model based on a local bond orientation scheme which reproduces the calculated results and is able to accurately predict the energies of arbitrary stacking sequences. This model has only two independent parameters, the energy of the intrinsic I_1 stacking fault and the energy difference between hcp and fcc Mg. Both energy and entropy considerations suggest that isolated I_1 stacking faults should predominate. [S0163-1829(97)04241-0]

I. INTRODUCTION

Stacking faults are common two-dimensional defects that occur when there is an error in the normal sequence of stacking of atomic layers. These faults may be formed during the growth process or created during a deformation process. Stacking faults are usually coupled to the existence of dislocations in the material. The mobility of the dislocations is governed in part by the energy of the stacking fault that is created in the wake of the motion, such as might be the case in the repulsion of two partial dislocations, or the shrinkage of a dislocation loop.[1]

In close-packed metals, such as hcp Mg or fcc Al, it is well known that planar defects are formed with relative ease, contributing to the ductile and malleable nature of these materials. The energies of these defects are usually small and an accurate measurement of these structures is often elusive. For example, the only known measurement[2] of the I_1 intrinsic stacking fault of Mg quotes a result of 60–150 erg cm^{-2}. However, it has been shown recently that theoretical modeling of close-packed metals based on local density theory gives reliable estimates of these energies, and in many instances the calculated energies might be considered more accurate than the exisiting experimental numbers. Theoretical studies of stacking faults are attractive owing to the ideal nature of the defect systems: atomic and volume relaxations are often negligible since in most instances the atoms in the faulted region maintain the close-packed coordination.[3–14]

The simple (111) stacking faults of both hcp and fcc metals can be described by a sequence of planes labeled by A, B, and C in the usual notation corresponding to the three possible atomic positions in a (111) plane. For the ideal hcp structure, this sequence is $\cdots ABABAB \cdots$ and $\cdots ABCABC \cdots$ for fcc. In different stacking sequences, some planes may have a local fcc-like environment, i.e., $A\dot{B}C$ stacking, where fcc-like planes are marked with a dot. In this notation, the intrinsic fault I_1, or growth fault, in the hcp structure can be formed by removing an A plane above the B plane, and then shearing the remaining planes above the B plane by the displacement $1/3[\bar{1}100]$:

$$I_1 \cdots ABABA\dot{B}CBCBCB \cdots .$$

Similarly, the intrinsic fault I_2, or deformation fault, can be formed by directly shearing the hcp lattice by the displacement $1/3[\bar{1}100]$:

$$I_2 \cdots ABABA\dot{B}\dot{C}ACACA \cdots .$$

The extrinsic stacking fault E is generated by inserting an extra C plane into the hcp stacking

$$E \cdots ABABA\dot{B}\dot{C}\dot{A}BABAB \cdots .$$

The (111) planes are the most frequently observed glide planes in hcp crystals, but they do not correspond to a twin. The T_2 fault is a competing low energy defect structure and is twinlike since it has mirror symmetry about the faulted plane:

$$T_2 \cdots ABABA\dot{B}C\dot{B}ABAB \cdots .$$

In this paper, we present results for these various stacking defects in hcp Mg calculated using a plane wave pseudopotential technique (described in Sec. II). The stacking fault supercells used and the convergence tests with respect to system size, sampling of the Brillouin zone, and atomic and

0163-1829/97/56(17)/10844(8)/$10.00

volume relaxations of the unit cell are discussed in Sec. III. Based on these calculated results, we construct a local bond orientation model in Sec. IV, and then use it to discuss the concentration of stacking faults in Sec. V.

II. METHOD

We use the plane wave pseudopotential method within the local density approximation (LDA) to solve the Kohn-Sham equations.[15,16] A detailed account of the iterative method used was given previously.[17] A crucial aspect of the algorithm as applied to metals is a subspace diagonalization which serves to orthogonalize the states, as well as to give the best estimate of the eigenstates of the Hamiltonian during the iteration to self-consistency. The states are occupied using a Fermi distribution function with a thermal broadening of 0.001 Hartree (approximately room temperature). The additional degree of freedom that arises in the determination of the occupation numbers results in an entropylike contribution to the energy that must be included to maintain the overall variational nature of the total energy functional.[18]

We use a separable pseudopotential[19] for Mg and a plane wave cutoff of 12 Ry for the expansion of the wave functions. Starting with unit vectors with additional random components as the initial guess to the wave functions, we attain self-consistency to better than 10^{-7} Hartrees without the instabilities reported by other iterative methods. We calculate the Hellmann-Feynman forces[20] and we then use a modified BFGS method[17,21] to relax the atomic displacements such that the forces on the atoms are less than $\sim 10^{-5}$ Hartree/Bohr. As we shall see in the next section, the atoms maintain the close-packed coordination in the faulted geometries, thus the relaxation energies are negligible.

The stacking fault energies are of the order of 10–40 meV and hence sensitive to the details of the Brillouin zone. Here, we construct systems of 12 and 16 atoms per unit cell, where the finite size of the Brillouin zone must be taken into account. In cases where the defect supercell and the bulk supercell are of the same size, as is the case for the intrinsic faults I_1 and I_2, we have used *identical* samplings of the zone in order to minimize errors. However, in the case of the extrinsic fault E, the perturbed system has an extra atom per cell compared with the bulk, thus requiring highly converged energies in terms of Brillouin zone integrations before we can accurately extract results. The **k** points were chosen according to the Monkhorst-Pack special points technique[22] and the point group symmetry of the lattice was used to reduce the number of independent **k** points. Even with this reduction, many special **k** points (110–426) are required, corresponding to 660 **k** points in the irreducible wedge for hcp Mg for the smallest **k** point sampling used. On the Intel Paragon parallel computer, the calculations associated with each **k** point were distributed to a separate node (up to 426 nodes).

III. RESULTS

A. Bulk magnesium

The calculated lattice parameters for hcp and fcc Mg obtained using 660 and 770 special **k** points in the irreducible wedges for the hcp and fcc structures, respectively, are given in Table I. The interlayer separation for hcp Mg ($z=\frac{1}{2}c/a$) is slightly smaller than the ideal value and is in reasonable agreement with experiment.[23]

TABLE I. The calculated in-plane lattice constant a and the (111) interplanar-spacing z for Mg in the hcp and fcc phases.

phase	a (Bohr)	z (units of a)
hcp	5.895	0.812
fcc	5.895	$\sqrt{\frac{2}{3}}=0.816$

We find the hcp phase to be lower in energy by 15 meV, which compares favorably with previous calculations.[24] (Since fcc Mg occurs at a larger volume and at a higher energy, a nonphysical negative pressure would be required to transform hcp Mg into fcc at zero temperature.) Since the hcp structure is lower in energy compared to fcc, to zeroth order, the ordering of the energies of the various stacking faults may be understood in terms of the number of fcc-like atoms in the sequence of (111) planes. But, as we will see in the next section, a simple one-parameter model that assigns an on-site energy to each fcc-like atom in the sequence does not describe the energetics of these systems quantitatively, and one needs to include local bond orientational effects to account for the results.

B. Stacking fault supercells

We use periodic supercells in our calculational scheme so that we necessarily have a finite number of layers in the stacking sequence. In doing so, we create additional faults in the supercell in some instances. It is imperative that these additional faults be, first, well separated so as to reduce the fault-fault interactions and, secondly, topologically identical to each other in order to be able to extricate the heat of formation of the defects from a single total energy calculation. With this in mind, we first considered supercells of 12 atoms per cell for the hcp, fcc, I_1, I_2, and T_2 structures; the E structure necessarily has an odd number of layers, so we choose 13 atoms per cell. In Table II we designate the actual supercells that we have used. Notice that the intrinsic supercells I_1 and I_2 have an extra identical fault in the calculational supercell. In all cases, we list the energy per fault of each system under consideration.

TABLE II. Number of atoms per cell, calculational supercell, number of faults per cell, and stacking fault energies (relative to hcp) for Mg. Locally fcc-like planes are denoted with a dot.

system	atoms	supercell	faults	energy (meV)
hcp	12	$ABABABABABAB$		0
fcc	12	$\dot{A}\dot{B}\dot{C}\dot{A}\dot{B}\dot{C}\dot{A}\dot{B}\dot{C}\dot{A}\dot{B}\dot{C}$		15
I_1	12	$ABABA\dot{B}CBCBC\dot{B}$	2	11
I_2	12	$ABABA\dot{B}\dot{C}ACA\dot{C}\dot{B}$	2	23
E	13	$ABABA\dot{B}\dot{C}\dot{A}BABAB$	1	36
T_2	12	$ABABA\dot{B}C\dot{B}ABAB$	1	27

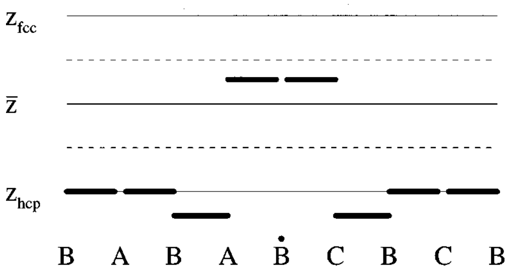

FIG. 1. The stacking sequence of planes around one of the two I_1 stacking faults in a 16 atom cell is denoted by A, B, C, with the fault plane marked with a dot. The vertical positions of the heavy horizontal lines connecting neighboring planes represent the values of the interlayer separation relative to the separations found in pure fcc ($z_{\rm fcc}$) and hcp ($z_{\rm hcp}$) stackings; $\overline{z}$ represents the Vegard's law value for the separation between an fcc-like plane and its first hcp-like neighbor.

C. Atomic and volume relaxations

The calculated in-plane lattice constants for both hcp and fcc Mg are the same, $a=5.895$ Bohr, but the fcc interplanar distance ($z_{\rm fcc}=0.816a$) is larger than the hcp value of $z_{\rm hcp}=0.812a$. Because the atoms in the faulted geometries maintain the close-packed coordination, we expect that there will only be interplanar atomic and volume relaxations along the $\hat{\mathbf{z}}$ direction in the defect systems; this assumption is supported by the small maximum force on the atoms in the ideal I_1 geometry of only 2.5×10^{-4} Hartree/Bohr. Simple Vegard's law arguments suggest an overall increase of the (111) length of the unit cell (relative to hcp) when a stacking fault exists and an expansion of the interplanar separation around those atoms that are locally fcc-like. The calculations bear out this expectation: the overall calculated increase in the supercell length agrees to $\sim$2% with the simple estimate, which is at the limit of the difference that can be meaningfully extracted. The calculated interlayer separations between neighboring planes around the fcc-like atom in a I_1 stacking fault are shown in Fig. 1 for a volume-relaxed (16 atom) supercell. If the simple Vegard's law arguments held, the separation between the fcc-like plane and its first neighbor would be $\overline{z}=\frac{1}{2}(z_{\rm fcc}+z_{\rm hcp})$; the actual separation is slightly larger, $\overline{z}+0.14\,(z_{\rm fcc}-z_{\rm hcp})$. This local expansion at the fault is then compensated by a decrease in the separation between the next-neighbor hcp-like planes relative to the expected value of $z_{\rm hcp}$ (see Fig. 1), but the separation of hcp-like planes further from the fault show no significant deviations from $z_{\rm hcp}$.

The energies associated with these relaxations are small; for the I_1 stacking fault, the total effect is $\sim$0.4 meV per fault. These relatively small relaxation energies do not affect the energies of the faults in any substantial way within the overall accuracy of the numbers, and are consistent with previous observations of stacking faults in Al.[9]

D. Finite size effects

The I_2 intrinsic stacking fault is most sensitive to the finite size of the unit cell since there are 4 fcc-like atoms per cell, more than in any of the other defect unit cells considered. The faults in the 12 atom supercell are separated by 3 and 5 atomic layers with the hcp region in between. We tested the dependence of the energies of the faults on the unit cell size by computing the energy in a 16 atom cell where the faults are periodically separated by 5 and 7 atomic layers in the $\hat{\mathbf{z}}$ direction. For completeness, we also computed the energy of the I_1 intrinsic fault in a 16 atom cell where the faults are equidistant from each other at 8 layers apart. Our results show that the 12 atom cell is adequate in describing the system of faults accurately since the energies agree to better than 1 meV with the results of the larger supercell.

E. Brillouin zone convergence

Finally in our convergence tests, we have investigated the dependence of the stacking fault energies on the sampling of the Brillouin zone. Here we have performed two tests. First, since the extrinsic stacking fault E necessarily has one extra atom per unit cell compared to the bulk,[25] we were compelled to derive highly converged *absolute* total energies with respect to Brillouin zone integrations in the $\hat{\mathbf{k}}_z$ direction. To this effect, we doubled the density of $\mathbf{k}$ points in the (111) direction for both the bulk hcp and faulted E structures, resulting in 426 special points for this low symmetry defect system. The total energy of the bulk and the faulted system remained unchanged to within 2 meV. As a second test, the planar sampling of the Brillouin zone was increased by 50% for the I_1 intrinsic stacking fault; the results using this more dense sampling agreed with the previous results to within 1 meV.

F. Discussion

Based on the convergence studies, the energies of the stacking faults listed in Table II appear to be converged to the order of 1–2 meV per fault with respect to system size, Brillouin zone integrations, and atomic and volume relaxations. The energies of these defects are small in comparison with stacking faults in fcc Al, which points to a high preponderance for Mg to be faulted. We have not considered the energy paths or the unstable stacking faults which are the barriers to the formation of these low-energy defects, but, based on our calculations, we suggest that Mg is likely to form stacking faults with the low energy I_1 and I_2 faults being the most probable defects.

Simon[3] reviewed various early theoretical estimates of the stacking fault energies for hcp Mg using simple pseudopotential theory. These estimates differ in the choice of potential, dielectric function, and whether the calculation is performed in real or reciprocal space. The quoted results fall in the range of 7–60 erg cm^{-2} for the I_1 stacking fault compared to our value of 21 erg cm^{-2}. These previous calculations were not self-consistent and thus are expected to have rather large uncertainities.

There are also large uncertainties in the experimental determination of the I_1 stacking fault. Using a kinetic modeling of the annealing of dislocation loops, Hales, Smallman, and Dobson[2,26] report energies of 60–150 erg cm^{-2} for the I_1 fault at 175 °C. A reanalysis[27] of the same data and using the same model—but without neglecting one term—reduced these values between 40% for the smaller values and 5% for the larger values of the stacking fault energies. These results, however, are still larger than our calculated value by almost a factor of 2. (For comparison, our calculated energies at zero temperature for the I_2, E, and T_2 faults, in the units of erg cm^{-2}, are 44, 68, and 51, respectively.)

Based on the previous successes of local density theory in predicting stacking fault energies, and given the convergence tests that we have performed, we believe that further experimental studies are needed. It has been argued that a direct measurement of the size of the dislocation loop is difficult for systems with fault energies greater than about 20 erg cm^{-2} since the fault widths are approximately inversely proportional to the stacking fault energy.[28] For systems with larger energies, one is compelled to assume a physical model—in this case, a model describing the dislocation loop shrinkage due to the surface which acts as a vacancy sink—to extract energies from direct experimental measurements. The difficulties with this procedure are compounded for Mg because the thin oxide layer at the surface acts instead as a source of vacancies. Analyzing the growth kinetics of double faulted loops, as was done in the measurement of Mg, introduces more uncertainties in the results.

IV. MODEL OF THE STACKING FAULT ENERGETICS

The system of faulted (111) planes in hcp Mg is a near ideal system. Since there are no substantial atomic and volume relaxations, the three-dimensional crystal may be modeled in terms of a one-dimensional sequence of planes labeled A, B, or C where no two subsequent atoms can be the same, thus neglecting the high-energy unstable stacking faults. Naively, such a simple system might be describable in terms of a model where the energetics of the system is due solely to the local environment, either hcp- or fcc-like.

The two possible local environments are shown in the top row of Fig. 2. An atom in the hcp-like environment will have an energy ε_1 and fcc-like atom will have an energy ε_2. The energy of an arbitrary sequence of atoms stacked in the (111) direction will have an energy of $(\varepsilon_2-\varepsilon_1)\times N_{\mathrm{fcc}}$ relative to the hcp structure, where N_{fcc} is the number of fcc-like atoms in the sequence.

The number of fcc-like atoms in I_1, I_2, E, and T_2 is 1, 2, 3, and 2, respectively, while the actual calculated energies of these faults are in the ratio of 1 : 2.1 : 3.3 : 2.5. While the ordering of the energies may be understood in these simple terms, this one-parameter model will give large quantitative discrepancies in attempting to predict the energetics of these systems.

To improve on this scheme, one could define a second-nearest-neighbor Ising model[29] that assigns a spin of $\sigma_j=+1$ to an atom j whose neighbor at $j+1$ is in the sequence of ABC, and $\sigma_j=-1$ to an atom whose neighbor at $j+1$ is in the sequence of CBA, where j labels the atoms in the sequence. The energy of such a system is then given by

$$E=J_1\sum_j \sigma_j\sigma_{j+1}+J_2\sum_j \sigma_j\sigma_{j+2}. \tag{1}$$

In the units of the coupling constants J_1 and J_2, the energies of the systems that we have considered are

$$E(\mathrm{fcc})=2J_1-2J_2 \quad (=15\ \mathrm{meV}), \tag{2}$$

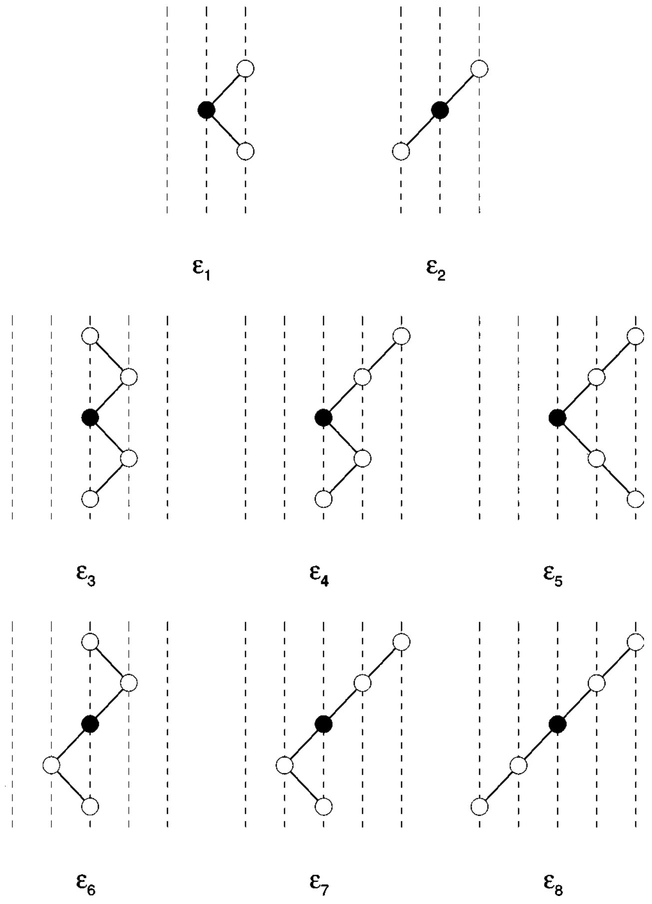

FIG. 2. Energy parameters associated with different local stacking sequences of (111) planes. For nearest-neighbors only, there are two interaction energies: ε_1 for the locally hcp-like and ε_2 for the locally fcc-like. The six distinct geometries for second-neighbor interactions are shown along with the corresponding energies ε_3 through ε_8.

$$E(I_1)=2J_1-4J_2 \quad (=11\ \mathrm{meV}), \tag{3}$$

$$E(I_2)=4J_1-4J_2 \quad (=23\ \mathrm{meV}), \tag{4}$$

$$E(E)=6J_1-4J_2 \quad (=36\ \mathrm{meV}), \tag{5}$$

$$E(T_2)=4J_1-8J_2 \quad (=27\ \mathrm{meV}). \tag{6}$$

For convenience, we have included, in brackets, our calculated results from section II that this model must be fitted to. Equations (2), (4) and (5) are consistent to within 2 meV with $2J_1=15$ meV and $4J_2=4$ meV. However, these parameters give unacceptably large discrepancies, predicting $E(I_1)=8$ meV and $E(T_2)=16$ meV. (The energy of the T_2 fault in this model is exactly twice that of the I_1 fault.) Improving this model by going to the third-nearest neighbor is not physical since we believe that the essential physics of this system must be captured in a model with short-range interactions.

A. Bond orientation model

Going beyond the model in which only the nearest-neighbor local environment—either hcp-like (H) or fcc-like

TABLE III. The local bond orientation scheme for atom j with nearest-neighbor atoms $j\pm 1$. H and F are atoms that are locally hcp-like or fcc-like, respectively. The parameters ε_3 to ε_8 have been fitted to the results in Table II.

$j-1$	j	$j+1$	Energy
H	H	H	$\varepsilon_3=0.0$ meV
H	H	F	$\varepsilon_4=1.0$ meV
F	H	F	$\varepsilon_5=6.6$ meV
H	F	H	$\varepsilon_6=9.0$ meV
H	F	F	$\varepsilon_7=9.8$ meV
F	F	F	$\varepsilon_8=14.3$ meV

(F)—is considered, leads to a model in which the energy of a site also depends on the local environment of the nearest neighbors, i.e., the relative (bond) orientation of neighboring planes. The physical basis for this model is that if the neighboring plane is hcp- (fcc-) like, then there is (not) direct bonding with the second-neighbor atoms. The six topologically distinct geometries that can occur are shown in Fig. 2 and summarized in Table III. The energies ε_3, ε_4, and ε_5 are ''ε_1 derived,'' and ε_6, ε_7, and ε_8 are ''ε_2 derived.'' Since fcc is higher in energy compared with hcp, we expect

$$\varepsilon_3<\varepsilon_4<\varepsilon_5<\varepsilon_6<\varepsilon_7<\varepsilon_8. \tag{7}$$

All energies are relative to hcp, so that there are five parameters in the model which can be fitted to the calculated energies. The model predicts the following expressions for the systems that we have considered thus far:

$$E(\text{fcc})=\varepsilon_8, \tag{8}$$

$$E(I_1)=2\varepsilon_4+\varepsilon_6, \tag{9}$$

$$E(I_2)=2\varepsilon_4+2\varepsilon_7, \tag{10}$$

$$E(E)=2\varepsilon_4+2\varepsilon_7+\varepsilon_8, \tag{11}$$

$$E(T_2)=2\varepsilon_4+\varepsilon_5+2\varepsilon_6. \tag{12}$$

Fitting to Eqs. (7)–(12), we determine the parameters listed in Table III. With this set, the energies listed in Table II are reproduced to within 1 meV. (The parameters must be given to tenths of a meV to avoid roundoff errors for configurations with large numbers of defects which would limit the predictive power of the model.) This model is effectively a second-neighbor model, but of a different type than considered earlier. If second neighbors were *not* correlated, then $\varepsilon_5-2\varepsilon_4=0$ since the shift of the second neighbors would be independent of each other. From the values of the parameters given in Table II, it is clear that this relationship does not hold.

The real test of this model, though, is its ability to predict the energies of other configurations. As a first test, we considered a hcp/fcc (111) interface in a 12 atom cell:

$$\text{interface}\qquad \dot{A}BABABA\dot{B}\dot{C}\dot{A}\dot{B}\dot{C}.$$

Using the model, the predicted energy for this structure is

$$E(\text{interface})=2\varepsilon_4+2\varepsilon_7+4\varepsilon_8=77\quad\text{meV}, \tag{13}$$

in good agreement with the first-principles calculated result (using 213 special **k** points) of 78 meV.

For all the test calculations we have considered, the energies predicted by the model agreed with the LDA results to within 2 meV. For example, the predicted energy for a randomly chosen structure denoted by $\dot{A}B\dot{A}\dot{C}\dot{B}\dot{A}\dot{C}BC\dot{B}\dot{A}C$, is $E=2\varepsilon_4+2\varepsilon_5+\varepsilon_6+4\varepsilon_7+3\varepsilon_8=106$ meV, while the calculated self-consistent result is 104 meV. These results demonstrate that this bond orientation model describes the energetics of arbitrary stacking faults quite well.

The relative values of ε_i, $i=3,\ldots,8$ suggest the additional relationships among the parameters

$$\varepsilon_5=\varepsilon_8-\varepsilon_6, \tag{14}$$

$$\varepsilon_7=\varepsilon_4+\varepsilon_6. \tag{15}$$

Furthermore, within this model, any stacking sequence will have only certain combinations of energy parameters. For example, going from an hcp region to a fault region will always add in contributions of either $\varepsilon_4+\varepsilon_6$ or $\varepsilon_4+\varepsilon_7$. By considering all distinct configurations possible, it is easy to show that the only two (nonzero) independent combinations of parameters necessary to describe a given packing sequence are

$$\varepsilon_8=14.6\ \text{meV}, \tag{16}$$

$$E[I_1]=2\varepsilon_4+\varepsilon_6=11.0\ \text{meV}, \tag{17}$$

where we have used the calculated values for these energies without further fitting. With these parameters, the originally calculated stacking fault energies are again reproduced to about 1 meV, while the agreement with the more complicated systems is 1–3 meV. (This simplified model predicts $E[I_2]=2E[I_1]$, although the calculated values differ by about 1 meV. Since energy differences of this order are within the overall accuracy limits, this is not a severe limitation of the model.) This simplified model suggests that the energetics of the stacking faults in Mg can be understood almost entirely by the energetics of the hcp-fcc energy difference and the intrinsic I_1 stacking fault energy.

B. Discussion

The stacking fault with the lowest energy is the simple I_1 fault. Using the models developed above, we find that isolated I_1 faults will always be favored compared to other configurations having the same number of faulted planes. The movement of stacking faults in a real material will proceed along, for example, edge dislocations, and will be limited by the diffusion barriers between different stackings. Assuming we have dislocations that can facilitate the shifting of planes, we can make several observations. If a single A plane is shifted (within an hcp $\cdots AB \cdots$ region) to a C plane, a T_2 fault is formed. Since this fault is significantly higher in energy than the separated I_1 faults, the T_2 fault should decay into two I_1 faults. Conversely, if two I_1 faults exist, there is a barrier to annihilation associated with the T_2 fault. Similarly, extrinsic E stacking faults should decay into I_1 and I_2 faults.

These energy considerations alone do not determine the distribution and concentration of stacking faults. To crudely

TABLE IV. The distinct configurations for $n \leqslant 3$ fcc-like planes in a crystal section containing N layers and M atoms per layer; the number of equivalent configurations $D(C)$; and the energies of the stacking sequence $E(C)$ in terms of the parameters $E(I_1)$ and ε_8. The values for general n for a pure fcc region and for separated defects are also given.

n	Configuration	$D(C)$	$E(C)/M$
0	$\cdots$ H$\cdots$	1	0
1	$\cdots$ F$\cdots$	N	$E(I_1)$
2	$\cdots$ FF$\cdots$	$N-1$	$2E(I_1)$
	$\cdots$ FHF$\cdots$	$N-2$	$E(I_1)+\varepsilon_8$
	$\cdots$ F$\cdots$ F$\cdots$	$\frac{1}{2}(N-2)(N-3)$	$2E(I_1)$
3	$\cdots$ FFF$\cdots$	$N-2$	$2E(I_1)+\varepsilon_8$
	$\cdots$ FFHF$\cdots$	$2(N-3)$	$2E(I_1)+\varepsilon_8$
	$\cdots$ FHFHF$\cdots$	$N-4$	$E(I_1)+2\varepsilon_8$
	$\cdots$ FF$\cdots$ F$\cdots$	$(N-3)(N-4)$	$3E(I_1)$
	$\cdots$ FHF$\cdots$ F$\cdots$	$(N-4)(N-5)$	$2E(I_1)+\varepsilon_8$
	$\cdots$ F$\cdots$ F$\cdots$ F$\cdots$	$\frac{1}{6}(N-4)(N-5)(N-6)$	$3E(I_1)$
n	$\cdots$ FF–F–FF$\cdots$	$N-(n-1)$	$2E(I_1)+(n-2)\varepsilon_8$
	$\cdots$ F$\cdots$ F$\cdots$ F$\cdots$	$\binom{N-2(n-1)}{n}$	$nE(I_1)$

include the temperature dependence, we consider the thermodynamics of a one-dimensional model of stacking faults in which we include the energetics and the configurational entropy associated with different stackings. The thermodynamical quantities as a function of temperature T ($\beta = 1/k_B T$) can be determined from the partition function

$$Z = \sum_{C} e^{-\beta E(C)}, \tag{18}$$

where $E(C)$ is the energy of a given configuration C. The probability of a configuration to occur is then simply given by

$$\rho(C) = \frac{1}{Z} e^{-\beta E(C)}. \tag{19}$$

Consider a section of a crystal with N layers and M atoms per layer, where each plane may be represented by either H or an F representing its local environment. For the model of the energetics developed above, fcc-like atoms separated by two or more hcp-like atoms are effectively independent. Making use of these assumptions, all allowed configurations and their energies can be calculated; the energies and number of equivalent configurations for $n \leqslant 3$ fcc-like planes are given in Table IV. The effect of more defects per configuration could be included by extending the results to higher n in a straightforward manner. (The general case results for separated faults and for a pure fcc region are also given in Table IV.) Conversely, an estimate of the contribution from all configurations with more defects can be made by noting that the energy of any configuration with n fcc-like sites is greater than $M \times nE(I_1)$ and there are $\binom{N}{n}$ such states with this energy. This contribution to the partition function for $n > 3$ can then be summed analytically and provides an upper bound to the actual contribution. As long as this estimate is significantly smaller than the contributions to the partition function from $n \leqslant 3$, the errors made by approximating the energy of these configurations by $nE(I_1)$ are neglible.

In Fig. 3, the concentrations of total fcc-like planes, and the concentration of fcc-like planes that are in clusters, are shown for two different numbers of atoms per plane ($M = 100$, 150) as a function of temperature. For the values of M shown, the contributions to the partition function from $n > 3$ were found to be small; the results with and without the $n > 3$ contributions are indistinguishable in the figure. Similarly, the results for different values of N (1000–10^5) are also indistinguishable, suggesting that these results are indicative of the thermodynamical limit. The first observation is that the concentration of fcc-like planes is small at room

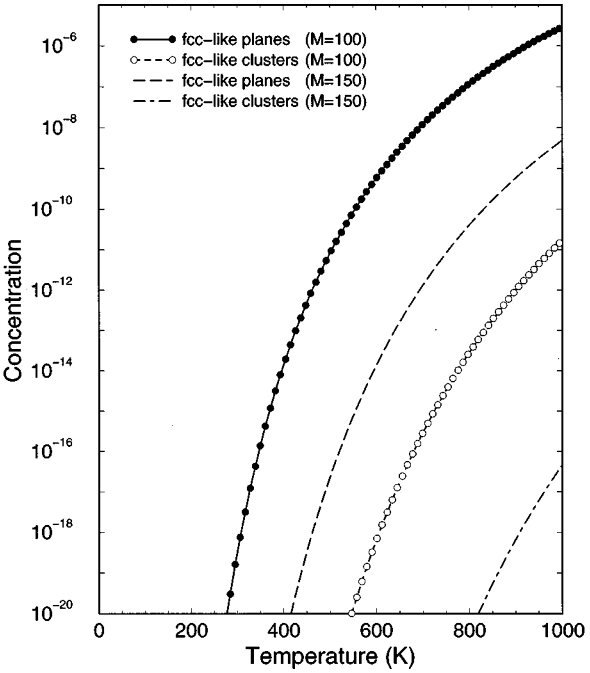

FIG. 3. Concentration of total fcc-like planes and of fcc-like planes in stacking fault clusters (for 100 and 150 atoms per layer) as a function of temperature. Contributions to the partition function for $n > 3$ are included.

temperature, but depends strongly on the value of M. This strong variation occurs because the energy of a configuration $E(C)$ is directly proportional to the number of faulted atoms $(M\times n)$ in the system, which in turn has an exponential effect on the contribution to the partition function. More explicitly, we can obtain an approximate upper bound to the concentration, c, of fcc-like planes as a function of M by again noting that $E(C)\leqslant M\times nE(I_1)$ for all n; the upper bound is simply

$$c(M)=[e^{\beta ME(I_1)}+1]^{-1}. \tag{20}$$

At room temperature, this equation predicts an upper bound to the concentration of fcc-like planes of 10^{-6} for $M=30$ verus the (unphysical) value of 10^{-100} for $M=500$, demonstrating the rapid change with M. Thus, the expected lateral dimensions of the fault regions in a real crystal are rather small.

Including the configurational entropy associated with atomic disorder in the plane will favor smaller M, but then the energy costs of the defects will favor larger M values. For values of M much smaller than ~ 100, the energetics may not be well described by the parametrization in terms of $E(I_1)$ and ε_8, nor will the configuration entropy be adequately described by the simple one-dimensional approach.

As already expected from energy considerations alone, there is no significant tendency for the fcc-like planes to cluster; the concentration of fcc-like atoms in stacking fault complexes is several orders of magnitude less than in separated faults (see Fig. 3). This behavior can be understood from the results in Table IV: the number of configurations for separated fcc planes is of the order of N times larger than any of the clusters. Thus, entropy considerations will favor separated I_1 faults.

V. CONCLUSIONS

We have studied the low-energy planar stacking fault defects in hcp Mg using first-principles local density approximation calculations. The convergence tests of finite size effects, Brillouin zone integrations, and atomic and volume relaxations suggest that the values are converged to within 2 meV. The absolute magnitude of the stacking fault energies are small, on the order of k_BT at room temperature. While these numbers are significantly smaller than those inferred from experiment, we suggest that the modeling used to deduce the experimental numbers may need to be reexamined.

The I_1 and I_2 intrinsic faults are found to be the most stable and to have a lower energy cost per atom than ideal fcc Mg. Based on the first-principles results, we construct a local bond orientation model of the stacking fault energetics that can accurately predict the self-consistently calculated energies. This model, with little loss in accuracy, can be reduced to two independent parameters, namely the energy of the I_1 stacking fault and the fcc-hcp energy difference. While this model is useful in discussing the thermal equilibrium properties of stacking faults, the actual dynamics and concentration of stacking fault motion will require the determination of far more complicated defect structures, which include dislocations and site disorder in the planes.

ACKNOWLEDGMENTS

We are grateful to G. Castilla and P. Thomas for discussions. The work at Brookhaven was supported by the Division of Materials Sciences, U.S. Department of Energy, under Contract No. DE-AC02-76CH00016, by a grant of computer time at the National Energy Scientific Computing Center, and the support of the Department of Energy High Performance Computing and Communications Program.

---

*Permanent address.

[1] J. P. Hirth and J. Lothe, *Theory of Dislocations* (Wiley, New York, 1982).

[2] R. E. Smallman and P. S. Dobson, Metall. Trans. **1**, 2383 (1970).

[3] J. P. Simon, J. Phys. F **9**, 425 (1979).

[4] S. Crampin, K. Hampel, D. D. Vvedensky, and J. M. MacLaren, J. Mater. Res. **5**, 2107 (1990); S. Crampin, D. D. Vvedensky, and R. Monnier, Philos. Mag. A **67**, 1447 (1993); J. M. MacLaren, A. Gonis, and G. Schadler, Phys. Rev. B **45**, 14 392 (1992).

[5] A. F. Wright, M. S. Daw, and C. Y. Fong, Philos. Mag. A **66**, 387 (1992); A. F. Wright and S. R. Atlas, Phys. Rev. B **50**, 15 248 (1994).

[6] P. J. H. Denteneer and J. M. Soler, J. Phys.: Condens. Matter **3**, 8777 (1991).

[7] J.-H. Xu, W. Lin, and A. J. Freeman, Phys. Rev. B **43**, 2018 (1991).

[8] N. M. Rosengaard and H. L. Skriver, Phys. Rev. B **47**, 12 865 (1993); **50**, 4848 (1994), and references therein.

[9] B. Hammer, K. W. Jacobsen, V. Milman, and M. C. Payne, J. Phys.: Condens. Matter **4**, 10 453 (1992).

[10] Q. Jin, P. Wang, D. Ding, and D. Wang, Phys. Lett. A **174**, 437 (1993).

[11] S. Schweizer, C. Elsässer, K. Hummler, and M. Fähnle, Phys. Rev. B **46**, 14 270 (1992); S. Schweizer, C. Elsässer, and M. Fähnle, *ibid.* **48**, 14 706 (1993).

[12] H. Teichler and S. Sanguinetti, Phys. Status Solidi A **138**, 361 (1993); A. Gross and H. Teichler, Philos. Mag. B **64**, 413 (1991).

[13] B. Pitveteau, M. C. Desjonquères, and D. Spanjaard, J. Phys. (France) **2**, 1677 (1992).

[14] K. Stokbro and K. W. Jacobsen, Phys. Rev. B **47**, 4916 (1993).

[15] P. Hohenberg and W. Kohn, Phys. Rev. **136**, B864 (1964); W. Kohn and L. J. Sham, *ibid.* **140**, A1133 (1965).

[16] S. H. Vosko, L. Wilk, and M. Nusair, Can. J. Phys. **58**, 1200 (1980).

[17] N. Chetty, M. Weinert, T. S. Rahman, and J. W. Davenport, Phys. Rev. B **52**, 6313 (1995).

[18] M. Weinert and J. W. Davenport, Phys. Rev. B **45**, 13 709 (1992).

[19] N. Troullier and J. L. Martins, Phys. Rev. B **43**, 1993 (1991); L. Kleinman and D. M. Bylander, Phys. Rev. Lett. **48**, 1425 (1982).

[20] R. P. Feynman, Phys. Rev. **56**, 340 (1939); H. Hellmann, *Einfuhrung in die Quantumchemie* (Deuticke, Leipzig, 1937).

[21] D. F. Shano, Math. Op. Res. **3**, 244 (1978).

[22] H. J. Monkhorst and J. D. Pack, Phys. Rev. B **13**, 5188 (1976).

[23] P. Villars and L. D. Calvert, *Pearson's Handbook of Crystallographic Data for Intermetallic Phases* (American Society for

Metals, Metals Park, OH, 1985).

[24] R. M. Wentzcovitch and M. L. Cohen, Phys. Rev. B **37**, 5571 (1988).

[25] Alternately, we could have constructed a system cell with an even number of atoms, but with two extrinsic faults per cell. These would have been three layers apart in a 12 atom supercell.

[26] R. Hales, R. E. Smallman, and P. S. Dobson, Proc. R. Soc. London, Ser. A **307**, 71 (1968).

[27] H. P. Leighly, Philos. Mag. **22**, 209 (1970).

[28] R. E. Beisser, Phys. Rev. B **8**, 5432 (1973).

[29] C. Cheng, R. J. Needs, and V. Heine, J. Phys. C **21**, 1049 (1988).